Eustatic change modulates exhumation in the Japanese Alps

Georgina E. King[1*], Floriane Ahadi[2], Shigeru Sueoka[3], Frédéric Herman[1], Leif Anderson[1], Cécile Gautheron[2], Sumiko Tsukamoto[4], Nadja Stalder[1], Rabiul Biswas [1,5], Matthew Fox[6], Guillaume Delpech[2], Stéphane Schwartz[7] and Takahiro Tagami[8]

[1]University of Lausanne, Institute of Earth Surface Dynamics, 1015, Lausanne, Vaud, Switzerland
[2]Université Paris-Saclay, CNRS, GEOPS, 91405, Orsay, France
[3]Japan Atomic Energy Agency, Tono Geoscience Center, Jorinji Izumichu, 509-5102, Japan
[4]Leibniz Institute for Applied Geophysics, 30655 Hannover, Germany
[5]Indian Institute of Technology Kanpur, Department of Earth Sciences, Kanpur-208016, India
[6]University College London, Earth Sciences, London, WC1E 6BT, UK
[7]Université Grenoble Alpes, ISTERRE, 38610, Gières, France
[8]Graduate School of Science, Kyoto University, Kyoto, 606-8502, Japan
*georgina.king@unil.ch

Abstract

The exhumation of bedrock is controlled by the interplay between tectonics, surface processes and climate. The highest exhumation rates of cm/yr are recorded in zones of highly active tectonic convergence such as the southern Alps of New Zealand or Himalayan syntaxes, where high rock uplift rates combine with very active surface processes. Here, by using a combination of different thermochronometric systems including trapped-charge thermochronometery, we show that such rates also occur in the Hida Mountain Range (HMR), Japanese Alps. Our results imply that cm/yr rates of exhumation are more common than previously thought. Our thermochronometry data allow the development of time-series of exhumation rate changes at the timescale of glacial-interglacial cycles and show a four-fold increase in baseline rates to rates of ~10 mm/yr within the past ~65 kyr. This increase in exhumation rate is likely explained by knickpoint propagation due to a combination of very high precipitation rates, climatic change, sea-level fall, range-front faulting and moderate rock uplift. Our data resolve cm scale sub-Quaternary exhumation rate changes showing that in regions with horizontal convergence, coupling between climate, surface processes and tectonics can exert a significant and rapid effect on rates of exhumation.

Introduction

The topography of mountain ranges evolves in response to rock uplift and erosion by climatically modulated surface processes, which together determine rates of rock exhumation. The highest bedrock exhumation rates are reported for actively converging mountains such as the southern Alps of New Zealand, Taiwan or the Himalayan syntaxes. Models predict that in rapidly uplifting orogens, the response time of erosion to climatic change is short (Whipple et al., 1999). However, direct measurements are lacking, in part because of the temporal mismatch between climatic changes and tectonic timescales. Here we show that cm/yr exhumation rates may be more common than previously thought and that coupling between tectonics and surface processes can profoundly modify rates of exhumation. We do this through applying a range of different thermochronometric methods that have different thermal sensitivities and thus record different stages of rock cooling throughout exhumation. The recently established set of trapped-charge thermochronometry methods (Guralnik et al., 2015; King et al., 2020) are sensitive to changes in exhumation at the timescale of glacial/interglacial cycles, allowing the response time of erosion to such climate transitions to be resolved.

The Japanese Alps reach elevations of 3,000 m, bisect the main Japanese island of Honshu and are thought to have formed ~3 Myr ago (Harayama et al., 2003; Sueoka et al., 2016) in response to convergence between the Philippine Sea Plate (PSP) and Amur Plate (Townend and Zoback, 2006). Strain partitioning along the Tokai-south Kanto block (Mazzotti et al., 2001, Fig. 1a) results in maximum deformation being accommodated in the northern Japanese Alps, corresponding to WNW-ESE shortening of 100-200 x 10^{-9}/yr (Mazzotti et al., 2001; Townend and Zoback, 2006). The HMR is the most northern and most extensive of the Japanese Alps, and was uplifted in two stages following volcanism in the late Pliocene, 2.7-1.5 Myr ago (Harayama et al., 2003; Oikawa, 2003), magmatism (Ito et al., 2021) and E-W compression since the Pleistocene, 1.4-0.5 Myr ago (Oikawa, 2003). High water availability and high heat flow caused by subduction of the PSP causes crustal weaking and focuses deformation in this region (Townend and Zoback, 2006). Partially molten rock, inferred from low seismic wave velocity zones, is thought to occur at depths of 12-20 km and 2-4 km beneath the HMR (Masubara et al., 2000), consistent with active magmatism resulting in regional topographic bulging and rock uplift (Townend and Zoback, 2006). Geodetic surveys indicate contemporary rock uplift rates of the HMR of 3-5 mm/yr (El-Fiky and Kato, 2006), comparable to catchment-averaged denudation rates of ~4 mm/yr (Fujiwara, 1999; Korup et al., 2014). The Kurobe catchment of the HMR has been estimated to yield the highest erosion rates in Japan (Yoshikawa, 1974).

Our study area is the Kurobe gorge, one of the steepest gorges in Japan. The Kurobe gorge descends 1 km over 5 km distance and is drained by the 85 km long Kurobe River, which discharges 1.8 km^3/yr of water into the Toyama basin and transported 1-2 Mt/yr of coarse sediment (sand and gravels) before the river was dammed (Uda and Omata, 1989). The HMR is one of the snowiest places on Earth, with a total annual precipitation of 4000 mm/yr (Uda and Omata, 1989) and annual snowfall between November and April of >9 m/yr. Peak snowmelt occurs in mid-April (Yamanaka et al., 2012) although peak discharge measured at the Kurobe dam usually occurs in the summer months (Wada et al., 2004) following convective rainfall. Multiple granitic intrusions have been recognized within the Kurobe region, ranging from >50 Ma in age to the ~0.8 Ma Kurobegawa granite, which has recently been shown to be the youngest surface-exposed granite yet-dated on Earth (Ito et al., 2013). Geobarometry data show that granites in the Kurobe region were emplaced at 4-10 km depth (Yamaguchi et al., 2003). The presence of the Kurobegawa granite at the surface, together with preliminary thermochronometric data (Yamada, 1999; Ito et al., 2013; King et al., 2020) and dam-sedimentation rates (Fujiwara et al., 1999; Esmaeili et al., 2015), indicate very high rates of erosion in this region, although the cause of these rates remains unclear.

Methods

Samples of granite were taken to form an elevation transect, along the main trunk of the Kurobe River and a tributary catchment, whilst three additional samples were taken from farther East, from Mt. Karamatsu and Mt. Kashimayarigadake (Fig. 1). We combined 12 new zircon (U-Th)/He ages (ZHe) and 11 new feldspar multi-OSL-thermochronometry ages with existing thermochronometric data (Fig. 2; Yamada, 1999; Ito et al., 2013; King et al., 2020). Infra-red-stimulated-luminescence measurements were made at 50, 100, 150 and 225 °C, allowing the different thermal stabilities of the luminescence signals to be exploited; as the IRSL 50°C data were in athermal steady-state, they were not included in the analyses. We combined the thermochronometric data using a 1-D thermal model (Biswas et al., 2018), which allows the generation of a time-series of exhumation rate changes (Fig. 3). To understand the causes of exhumation rate changes in Kurobe, we use stream-power modelling to track the migration of knick-points throughout the catchment (Fig. 4; Schwanghart and Scherler, 2014) and evaluate the glacial history of the catchment by estimating the equilibrium line altitude from climate records (Anderson et al., 2021). Full methodological details are given in the Supplementary Materials.

Exhumation rates

In agreement with existing thermochronometric data, the OSL and ZHe ages obtained are extremely young, yielding minimum ages of 8 ka and 0.1 Ma respectively for samples from the main river valley (Figs. 1 and 2). The combined conversion of the ZFT and ZHe data into exhumation rates yields a rate of <0.2 mm/yr until 2.5 Ma when rates increase, reaching ~2 mm/yr at around 1 Ma (Fig. 3a). Rates peak at 6-14 mm/yr within the past 0.3 Myr (Fig. 3a). In contrast, samples from the East of the HMR from Mt. Karamatsu and Mt. Kashimayarigadake reveal peak exhumation of 6 mm/yr around 4 Ma and rates of <0.2 mm/yr since 2 Ma (Fig. 1 and 3a). Performing the same exercise using the OSL and electron spin resonance (ESR) data reveals a complex exhumation rate history over the past 0.15 Myr (Fig. 3b and 3c), resolved because of the sensitivity of trapped-charge dating systems over kyr timescales. Whereas samples from the main Kurobe River exhumed rapidly with rates of >10 mm/yr over the past ~20 kyr, samples from the tributary catchment exhumed rapidly with rates of ~10 mm/yr around ~65 ka before reducing to rates of <5 mm/yr over the past 50 kyr (Figs. 3b, 3c, 4a).

The high rates of exhumation recorded for the study area are commensurate with rates elsewhere in the HMR (Spencer et al., 2019) but are anomalous relative to the Japanese Alps more generally (Korup et al., 2014; Yoshikawa, 1974). Ito et al. (2021) have proposed that intrusion of the Kurobegawa granite by three phases of magmatism at 2.1-2.0 Ma, ~1.0 Ma and 0.8-0.7 Ma resulted in uplift of the study area; contemporaneous with the increase in exhumation rates to ~2 mm/yr recorded by the ZHe and ZFT data (Fig. 3a).

The youngest granites are exposed in the main Kurobe River valley, coincident with the majority of samples that yield the most recent phase of rapid exhumation (Figs. 3, 4). However, the kyr timescale of exhumation rate changes revealed by the thermochronometric ages (Fig. 3) suggests that additional processes drive erosion rate changes in the Kurobe basin. We propose that the data are best explained by knickpoint propagation along the Kurobe River in response to the combined effects of eustatic changes, climate change, range-front faulting and magmatism induced uplift.

Knickpoint propagation

Knickpoints are a change in channel slope and form in river valleys in response to spatially-variable tectonic uplift, base-level change, and/or fault activity (Whipple and Tucker, 1999; Steer et al., 2019). Rapid knickpoint retreat occurs in catchments with high stream-power and bedload transport (Cook et al., 2013). The large volumes of sediment mobilised in the Kurobe catchment are documented both by rapid rates of dam sedimentation (Esmaeili et al., 2015) and also by the extensive 120 km^2 Kurobe alluvial fan. Uplift of the HMR, range-front faulting, subsidence of the Toyama basin and climatically driven sea-level changes have caused the Kurobe River base-level to change extensively over the Quaternary. Sea level low-stands of up to ~140 m occurred in the Japan Sea during the Late Pleistocene (Oba and Irino, 2012) and the combination of eustatic change and uplift means that the Kurobe River base-level has increased by ~80 m in the past 10 kyr (Ishikawa, 1991). Calculation of the normalised channel steepness, a simplified proxy of river stream power, reveals peak values around the study site (Fig. 4a). The combination of high base level change, high channel steepness and high sediment transport mean that during sea-level low stands, rapid bedrock incision and knickpoint propagation occurred at the sample location.

Multiple knickpoints occur in the catchment including between the main Kurobe River and the sampled tributary channel (Fig. 4b) where the river profile is over-steepened. This feature may relate to a change in lithology between different granitic intrusions (Fig. 1b), to localised faulting (Ito et al., 2013), or to knickpoint formation during glacial period sea-level low-stands and subsequent upstream knickpoint propagation. Analysis of the river profile indicates that the most significant knickpoint is coincident with the Kurobe dam around 10 km upstream of the study area (Supplementary Material). Whilst the dam conceals the true scale of the knickpoint, steepening of the river channel indicates a minimum knickpoint elevation of 40 m. Assuming that this feature relates to base-level fall during the last glacial maximum (LGM), 20 kyr ago, basin-wide knickpoint propagation modelling (Crosby and Whipple, 2006) yields a knickpoint retreat rate of ~3 m/yr (Supplementary Material). Whilst this rate is high, the high sediment transport of the Kurobe River, coupled with its high discharge and steepness, plus sea-level fall of ~120 m during the LGM (Oba and Irino, 2012) mean that knickpoint retreat must have been rapid.

The difference in timing of peak exhumation revealed by the ESR and OSL data in the main river channel and the tributary valley (Fig. 3b and 3c) reflects more rapid rock cooling in the main channel. This likely relates to more significant exhumation of the main river channel, driven by its larger drainage area, but may also be influenced by hydrothermal activity related to emplacement of the Kurobe granite (Ito et al., 2013). Nevertheless, data from both locations yield a mean exhumation rate of ~9 mm/yr over 15 ka, equating to approximately 130 m of exhumation. Whilst ~40 m of this can be related to the continued uplift of the HMR, as revealed by geodetic surveys (El-Fiky and Kato, 2006), dam sedimentation rates (Fujiwara et al., 1999) and detrital cosmogenic nuclide data (Korup et al., 2014), and is consistent with the baseline rates of 2-4 mm/yr revealed by the ESR, OSL, ZFT and ZHe data (Fig. 3), the remainder likely relates to surface erosion and incision following base level change of the Kurobe River due to climatic changes over the past ~65 ka.

Glacial climate

In addition to eustatic change, enhanced erosion due to glacial or periglacial processes throughout the late Quaternary period will have also influenced the exhumation of Kurobe. The peak in exhumation rates of ~9 mm/yr at ~65 ka in the tributary catchment (Fig. 3b) is contemporaneous with MIS3/4 and what is thought to be the most extensive glaciation of Japan (Ono, 1991). Although global temperature was cooler during MIS2 than MIS3/4, more significant lowering of the Japan Sea level during MIS2 reduced moisture availability to the Japanese Alps preventing the establishment of large glaciers (Ono, 1991). During MIS4, the altitude of maximum ice extent in the HMR ranged from ~2,350 m in the West to ~1000 m in the East (Kawasumi, 2009), however equilibrium line altitude modelling using local climate records suggests that it is highly unlikely that Kurobe was glaciated at this time (Supplementary Material), indicating that periglacial processes were dominant.

The HMR is one of the snowiest places on Earth and under the cooler, humid conditions of MIS3/4 it is possible that annual snowfall exceeded the modern average of 9 m/yr (Aoki and Hasegawa, 2003). Periglacial processes coupled with enhanced stream power and fluvial incision following snowmelt may have increased sediment supply to the Kurobe River, further increasing erosion (Cook et al., 2013). After ~50 ka, estimated exhumation rates in the tributary catchment reduced to ~2 mm/yr, commensurate with present day rates (Korup et al., 2014; Fujiwara et al., 1999). We suggest that these rates are typical of interglacial periods and are likely controlled by a combination of precipitation and earthquake driven landsliding (Kariya et al., 2011), continued uplift due to E-W compression and magma injection.

Conclusions

The exhumation rates recorded in Kurobe are some of the highest recorded on Earth, implying that cm/yr rates of exhumation are more common than previously thought. Kurobe is a high strain setting, similar to e.g. the Southern Alps of New Zealand, where a combination of tectonic convergence and active magmatism result in high rates of uplift. It is debated whether tectonics or climate controls Cenozoic exhumation and the role of global climatic cooling is at the centre of the dispute (Molnar and England, 1990). Here, using a suite of thermochronometers, we show that climatically-modulated eustatic and surface process changes, coupled with tectonics, strongly controls exhumation rates over sub-Quaternary timescales.

Figure captions:

Fig. 1: Sample location and thermochronometric ages. (a) Tectonic setting and accommodation of Philippine Sea/Amur convergence (Mazotti et al., 2001). (b) Geological map showing key faults (solid lines) as well as zircon U-Pb ages, (Z(U-Pb)) (modified from Ito et al., 2003). (c) Zircon fission-track (Yamada, 1999; ZFT); (d) zircon helium (this study, ZHe), (e) optically stimulated luminescence (King et al., 2020 and this study; OSL) and (f) electron spin resonance (King et al., 2020; ESR) ages.

Fig. 2: Age-elevation relationship of the thermochronometric data. OSL data from King et al. (2020) and this study, ESR from King et al. (2020), ZFT from Yamada (1999) and Z(U-Pb)

from Ito et al. (2003). Uncertainties for the OSL and Z(U-Pb) data are within the size of the datapoints.

Fig. 3: Exhumation rates. Calculated from inversion of the thermochronometric data using a 1D thermal model (Biswas et al., 2018). (a) ZFT and ZHe data (b) OSL and ESR data of samples from the tributary valley and (c) from the main trunk of the Kurobe River; yellow and red sample-locations in Fig. 4a respectively. Shading highlights the timing of peak exhumation, with duration of ~15 ka; Marine Isotopic Stages (MIS) are indicated.

Fig. 4: Stream modelling of the Kurobe River. (a) The Kurobe River coloured according to channel steepness (k_{sn}), warmer colours indicate higher values. Sample locations are shown as filled circles. (b) Knickpoints (open circles) identified using the knickpoint finder function in TopoToolbox (Schwanghart and Scherler, 2014).

Acknowledgements

This research was supported by the Swiss National Science Foundation (PZ00P2_167960 to GEK) and the Grant-in-Aid for Scientific Research on Innovative Areas from the Ministry of Education, Culture, Sports, Science and Technology (MEXT) (KAKENHI 26109003 to SS/TT). We thank the Chubu Regional Environment Office for permission to collect rocks. Sample collection was supported by the Kansai Electric Power Co., Inc., Yasuhisa Hino (KANSO Co., Ltd.), Tetsuya Komatsu, Shuji Terusawa, Shoma Fukuda, Takayuki Arai and the staff of the Azohara lodge.

References

Aoki, T., Hasegawa, H., 2003. Late Quaternary glaciations in the Japanese Alps: controlled by sea level changes, monsoon oscillations and topography. Zeitschrift für Geomorphologie (Supplement “Glaciation and Periglaciation in Asian High Mountains”), 130, 195-215.

Cook, K.L., Turowski, J.M. and Hovius, N., 2013. A demonstration of the importance of bedload transport for fluvial bedrock erosion and knickpoint propagation. *Earth Surface Processes and Landforms*, *38*(7), pp.683-695.

Crosby, B.T. and Whipple, K.X., 2006. Knickpoint initiation and distribution within fluvial networks: 236 waterfalls in the Waipaoa River, North Island, New Zealand. *Geomorphology*, *82*(1-2), pp.16-38.

El-Fiky, G. and Kato, T., 2006. Secular crustal deformation and interplate coupling of the Japanese Islands as deduced from continuous GPS array, 1996–2001. *Tectonophysics*, *422*(1-4), pp.1-22.

Esmaeili, T., Sumi, T., Kantoush, S., Kubota, Y. and Haun, S., 2015, June. Three-dimensional numerical modeling of sediment flushing: case study of Dashidaira Reservoir, Japan. In *Proceedings of the 36th IAHR World Congress, The Hague, The Netherlands* (Vol. 28).

Fujiwara, O., Sanga, T., Ohmori, H., 1999. Regional distribution of erosion rates over the Japanese Islands. JNC Technical Review 5, 85-93 (in Japanese with English Abstract)

Guralnik, B., Jain, M., Herman, F., Ankjærgaard, C., Murray, A.S., Valla, P.G., Preusser, F., King, G.E., Chen, R., Lowick, S.E., Kook, M., Rhodes, E.J., 2015b. OSL-thermochronology of feldspar from the KTB Borehole, Germany. Earth and Planetary Science Letters 423, 232-243.

Harayama, S., Ohyabu, K., Miyama, Y., Adachi, H., Shukuwa, R., 2003. Eastward tilting and uplifting after the late Early Pleistocene in the eastern-half area of the Hida Mountain Range. Quaternary Research (Daiyonki Kenkyu) 42, 127-140. (in Japanese with English Abstract)

Ikeda, Y., 1996. The fact of topographical observation about the form of the Hida Mountains, Chikyu Monthly, 18, 62–76 (in Japanese).

Ishikawa, T. 1991. Sediment movement on the kurobe alluvial fan**.** Fluvial Hydraulics of Mountain Regions. Editor: Aronne Armanini, Giampaolo Di Silvio, Lecture Notes in Earth Sciences, vol. 37, p.195-207

Ito, H., Yamada, R., Tamura, A., Arai, S., Horie, K. and Hokada, T., 2013. Earth's youngest exposed granite and its tectonic implications: the 10–0.8 Ma Kurobegawa Granite. *Scientific reports*, *3*(1), pp.1-5.

Ito, H., Adachi, Y., Cambeses, A., Bea, F., Fukuyama, M., Fukuma, K., Yamada, R., Kubo, T., Takehara, M. and Horie, K., 2021. The Quaternary Kurobegawa Granite: an example of a deeply dissected resurgent pluton. Sci. Rep., 11, 22059.

Matsubara, M., Hirata, N., Sakai, S. and Kawasak, I., 2000. A low velocity zone beneath the Hida Mountains derived from dense array observation and tomographic method. Earth Planets Space, 52, 143-154.

Kariya, Y., Sato, G. and Komori, J., 2011. Landslide-induced terminal moraine-like landforms on the east side of Mount Shiroumadake, Northern Japanese Alps. *Geomorphology*, *127*(3-4), pp.156-165.

Kawase, H., Yamazaki, A., Iida, H., Aoki, K., Shimada, W., Sasaki, H., Murata, A., Nosaka, M., 2018. Simulation of Extremely Small Amounts of Snow Observed at High Elevations over the Japanese Northern Alps in the 2015/16 Winter, SOLA, 14, 39-45.

Kawasumi, T., 2009. Chronological significance of Tateyama E tephra on the lowest moraine (Iwatake Stage) on the eastern side of Mt. Shiroumadake, Hida Range, central Japan. Journal of Geography (Chigaku Zasshi) 118, 717-725. (in Japanese with English Abstract)

King, G.E., Tsukamoto, S., Herman, F., Biswas, R.H., Sueoka, S. and Tagami, T., 2020. Electron spin resonance (ESR) thermochronometry of the Hida range of the Japanese Alps: validation and future potential. Geochronology, 2(1), pp.1-1.

Korup, O., Hayakawa, Y., Codilean, A.T., Matsushi, Y., Saito, H., Oguchi, T. and Matsuzaki, H., 2014. Japan's sediment flux to the Pacific Ocean revisited. *Earth-science reviews*, *135*, pp.1-16.

Mazzotti, S., Henry, P., Le Pichon, X., 2001. Transient and permanent deformation of central Japan estimated by GPS: 2. Strain partitioning and arc-arc collision. Earth and Planetary Science Letters 184(2), pp.455-469.

Molnar, P. and England, P., 1990. Late Cenozoic uplift of mountain ranges and global climate change: chicken or egg?. *Nature*, *346*(6279), pp.29-34.

Oba, T. and Irino, T., 2012. Sea level at the last glacial maximum, constrained by oxygen isotopic curves of planktonic foraminifera in the Japan Sea. *Journal of Quaternary Science*, *27*(9), pp.941-947.

Oikawa, T., 2003. The Spatial and Temporal Relationship between Uplifting and Magmatism in the Hida Mountain Range, Central Japan. The Quaternary Research (Daiyonki-Kenkyu) 42, 141-156. (in Japanese with English Abstract)

Ono, Y., 1991. Glacial and periglacial paleoenvironments in the Japanese Islands. Quaternary Research (Daiyonki Kenkyu) 30, 203-211.

Schwanghart, W. and Scherler, D., 2014. TopoToolbox 2–MATLAB-based software for topographic analysis and modeling in Earth surface sciences. *Earth Surface Dynamics*, *2*(1), pp.1-7.

Spencer, C.J., Danišik, M., Ito, H., Hoiland, H., Tapster, S., Jeon, H., McDonald, B., Evans, N.J., 2019. Rapid exhumation of Earth's Youngest exposed granites driven by subduction of an Oceanic Arc. Geophysical Research Letters 46, pp.1259-1267.

Steer, P., Croissant, T., Baynes, E. and Lague, D., 2019. Statistical modelling of co-seismic knickpoint formation and river response to fault slip. *Earth Surface Dynamics*, *7*(3), pp.681-706.

Suoeka, S., Tsutsumi, H., Tagami, T., 2016. New approach to resolve the amount of Quaternary uplift and associated denudation of the mountain ranges in the Japanese Islands. Geoscience Frontiers 7(2), 197-210.

Townend, J., Zoback, M.D., 2006. Stress, strain, and mountain building in central Japan. Journal of Geophysical Research: Solid Earth (1978–2012) 111.

Uda T, and Omata A, 1989, A research report on sediment loss from coast to deep sea. *PWRI Report*, no. 2730, 80p. (in Japanese).

Wada, N., Kawada, R., Aoki, K, Kume, A., 2004. Increasing winter runoff in a middle-latitude mountain area of central Japan. *Journal of the Meteorological Society of Japan*, 82(6), pp.1589-1597.

Whipple, K.X. and Tucker, G.E., 1999. Dynamics of the stream-power river incision model: Implications for height limits of mountain ranges, landscape response timescales, and research needs. *Journal of Geophysical Research: Solid Earth*, *104*(B8), pp.17661-17674.

Yamada, R. 1999. Cooling history analysis of granitic rock in the Northern Alps central Japan. Earth Monthly (Gekkan Chikyu) 21, 80-810. (in Japanese)

Yamaguchi, Y., Wada, H., Ohta, Y., Harayama, S., 2003. Amphibole zoning, a record of progressive oxidation during crystallization of mafic microgranular enclaves in the Kurobegawa Granitic Pluton. Journal of Mineralogical and Petrological Sciences 98, 151-155.

Yamanaka, T., Wakiyama, Y. and Suzuki, K., 2012. Is snowmelt runoff timing in the Japanese Alps region shifting toward earlier in the year?. *Hydrological Research Letters*, *6*, pp.87-91.

Yoshikawa, T., 1974. Denudation and tectonic movement in contemporary Japan. *Bulletin of the Department of Geography, University of Tokyo*, *6*, pp.1-14.

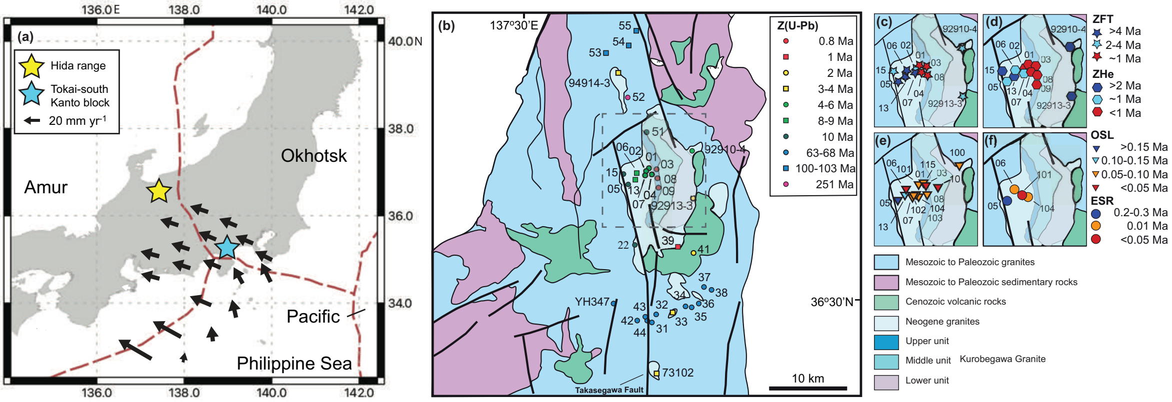
(a)
Hida range
Tokai-south Kanto block
20 mm yr-1
Amur
Okhotsk
Pacific
Philippine Sea
136.0E
138.0
140.0
142.0
40.0
38.0
36.0
34.0
40.0N
(b)
137°30'E
36°30'N
Z(U-Pb)
0.8 Ma
1 Ma
2 Ma
3-4 Ma
4-6 Ma
8-9 Ma
10 Ma
63-68 Ma
100-103 Ma
251 Ma
94914-3
92910-4
92913-3
YH347
73102
Takasegawa Fault
10 km
(c)
(d)
(e)
(f)
ZFT
>4 Ma
2-4 Ma
~1 Ma
ZHe
>2 Ma
~1 Ma
<1 Ma
OSL
>0.15 Ma
0.10-0.15 Ma
0.05-0.10 Ma
<0.05 Ma
ESR
0.2-0.3 Ma
0.01 Ma
<0.05 Ma
Mesozoic to Paleozoic granites
Mesozoic to Paleozoic sedimentary rocks
Cenozoic volcanic rocks
Neogene granites
Upper unit
Middle unit
Kurobegawa Granite
Lower unit

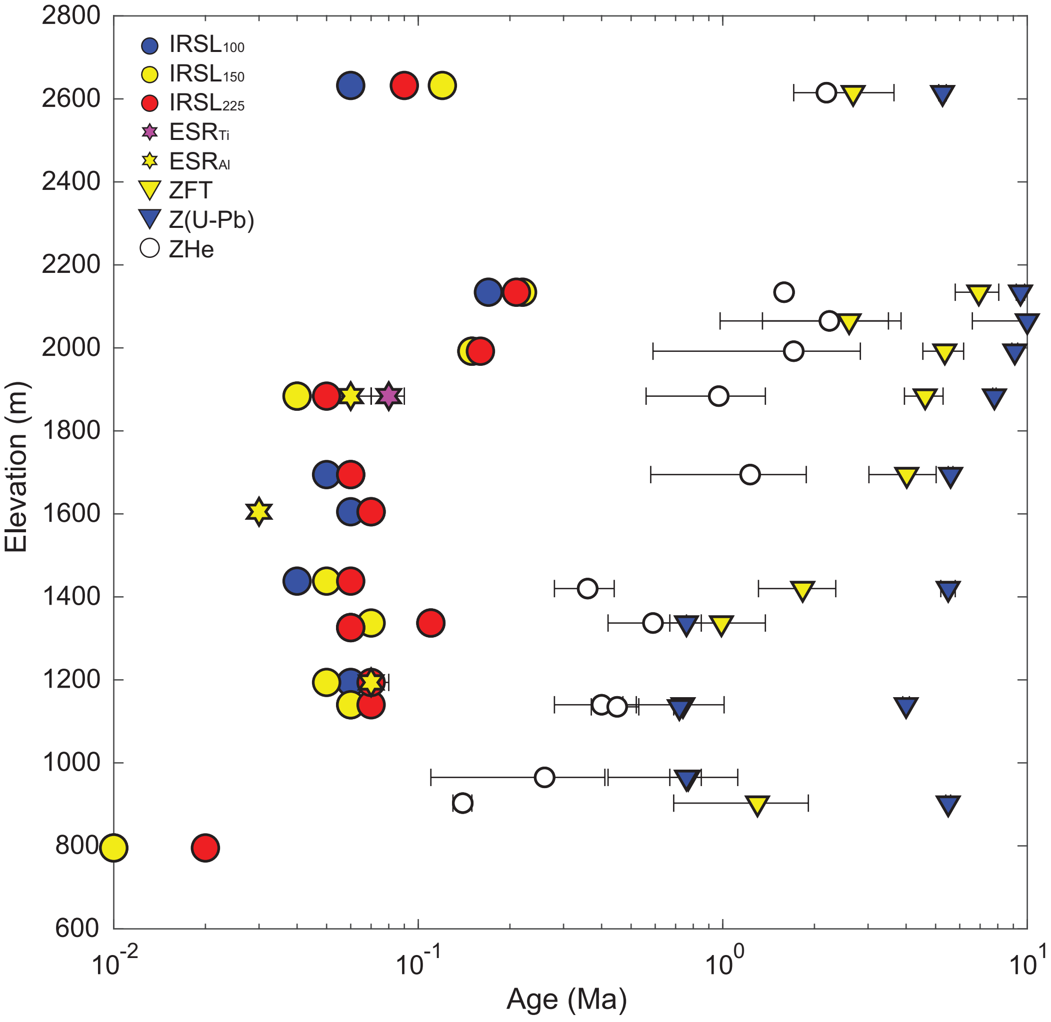
IRSL100
IRSL150
IRSL225
ESRTi
ESRAl
ZFT
Z(U-Pb)
ZHe
Elevation (m)
2800
2600
2400
2200
2000
1800
1600
1400
1200
1000
800
600
Age (Ma)
10-2
10-1
100
101

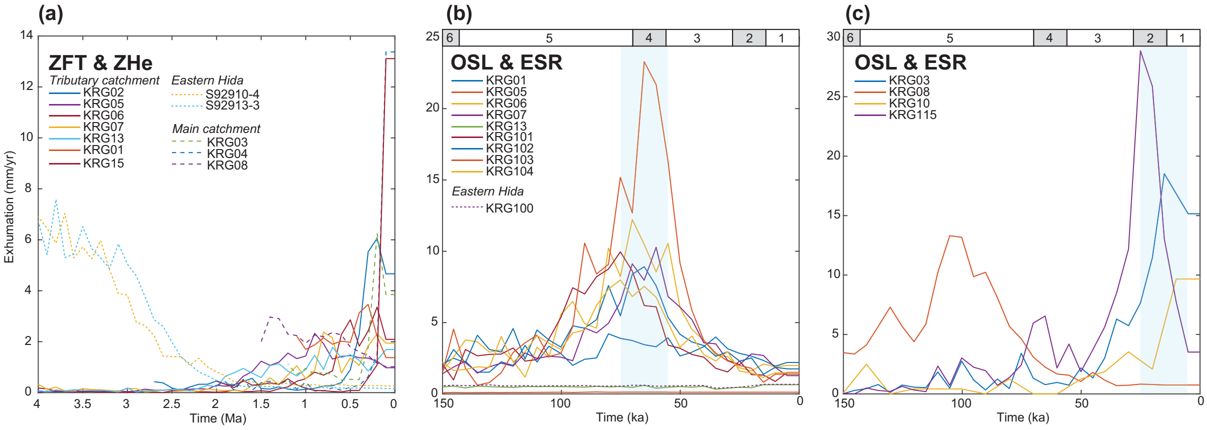
(a)
ZFT & ZHe
Tributary catchment
KRG02
KRG05
KRG06
KRG07
KRG13
KRG01
KRG15
Eastern Hida
S92910-4
S92913-3
Main catchment
KRG03
KRG04
KRG08
Exhumation (mm/yr)
Time (Ma)
0
2
4
6
8
10
12
14
4
3.5
3
2.5
2
1.5
1
0.5
0
(b)
OSL & ESR
KRG01
KRG05
KRG06
KRG07
KRG13
KRG101
KRG102
KRG103
KRG104
Eastern Hida
KRG100
6
5
4
3
2
1
0
5
10
15
20
25
150
100
50
0
Time (ka)
(c)
OSL & ESR
KRG03
KRG08
KRG10
KRG115
6
5
4
3
2
1
0
5
10
15
20
25
30
150
100
50
0
Time (ka)

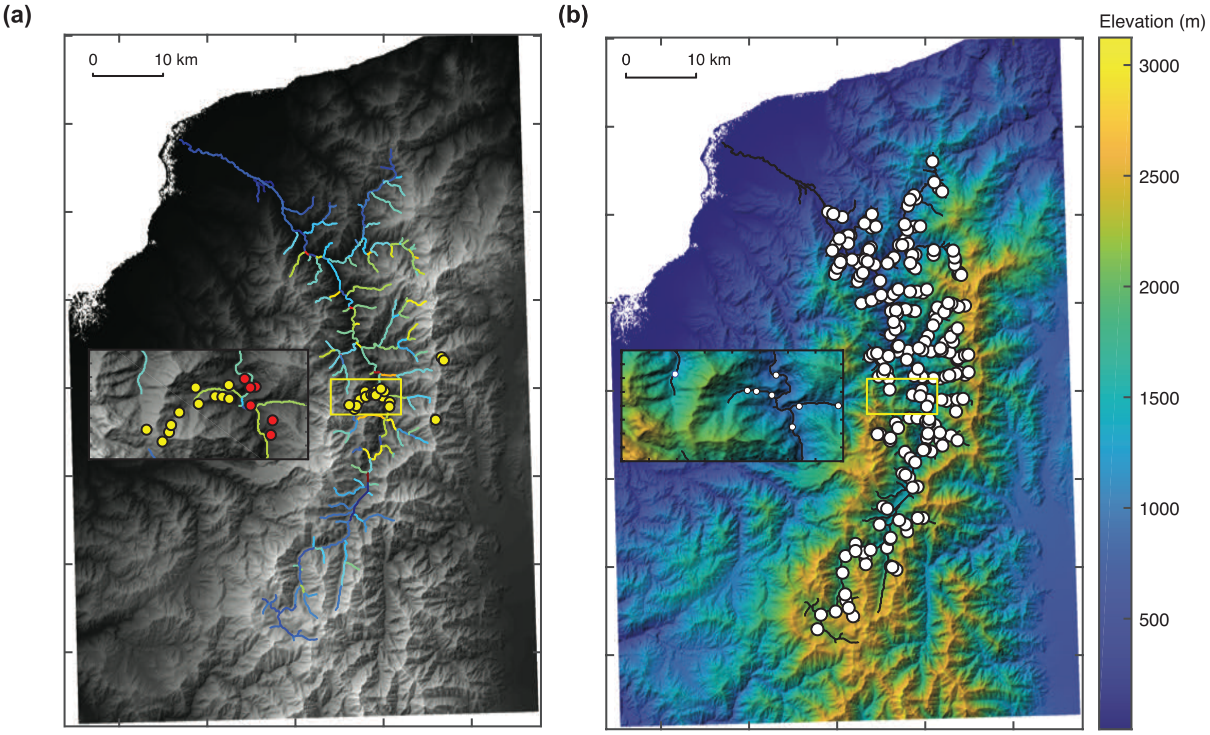
(a)
0
10 km
(b)
0
10 km
Elevation (m)
3000
2500
2000
1500
1000
500